

Spherical Thin-Shell Wormholes and Modified Chaplygin Gas

M. Sharif¹ *and M. Azam^{1,2} †

¹ Department of Mathematics, University of the Punjab,
Quaid-e-Azam Campus, Lahore-54590, Pakistan.

² Division of Science and Technology, University of Education,
Township Campus, Lahore-54590, Pakistan.

Abstract

The purpose of this paper is to construct spherical thin-shell wormhole solutions through cut and paste technique and investigate the stability of these solutions in the vicinity of modified Chaplygin gas. The Darmois-Israel formalism is used to formulate the stresses of the surface concentrating the exotic matter. We explore the stability of the wormhole solutions by using the standard potential method. We conclude that there exist more stable as well as unstable solutions than the previous study with generalized Chaplygin gas [19].

Keywords: Thin-shell wormholes; Darmois-Israel conditions; Stability.

PACS: 04.20.Gz; 04.20.-q; 04.40.Nr; 04.70.Bw.

1 Introduction

Wormhole physics has been an interesting subject for physicists since the first traversable wormhole by Morris and Throne as a solution of the Einstein field equations [1]. The fascinating idea was to connect two distinct or the same universe through a handel or tunnel [1, 2]. The main issue with this wormhole

*msharif.math@pu.edu.pk

†azammath@gmail.com

is the existence of inevitable amount of exotic matter around the throat. The problem of minimizing the usage of exotic matter for the physical viability of wormhole has received a considerable attention. For instance, it was shown that with suitable choice of wormhole geometry [3], it is possible to reduce exotic matter around the wormhole throat. Visser [2, 4] analyzed that the violation of energy condition could be minimized with the construction of thin-shell wormholes through cut and paste technique. This construction restricts exotic matter to be placed at the wormhole throat. The study of thin-shell wormholes with the Darmois-Israel formalism [5, 6] has widely been discussed in literature [7]-[10].

It is believed that any traversable wormhole is of physical interest if it is stable under linear perturbations preserving the spherical symmetry. In this scenario, many authors carried out the stability analysis of thin-shell wormholes through linear perturbations. Poisson and Visser [11] performed stability analysis for the Schwarzschild thin-shell wormholes. Afterwards, the same analysis was extended for charge [12] and cosmological constant [13]. It was found that the stability regions would be increased with the inclusion of charge and positive cosmological constant while decreased for the negative cosmological constant. The dilaton thin-shell wormholes with and without charge was investigated by different authors [14]. Eiroa and his collaborators [15] constructed cylindrical thin-shell wormholes and investigated their stability. Recently, we have explored the stability of spherical and cylindrical thin-shell wormholes under linear perturbations [16].

The choice of equation of state for the description of matter present in the wormhole throat has a great relevance in the existence and stability of wormhole static solutions. In this context, Eiroa and Simeone [17] constructed the spherical thin-shell wormholes with matter source as pure Chaplygin gas. They concluded that static stable and unstable wormhole solutions exist depending upon the parameters in the model. Bandyopadhyay et al. [18] generalized this analysis by considering simple modified Chaplygin gas and found that stable static wormhole solutions are also possible in the Schwarzschild as well as Schwarzschild de-Sitter cases. Later, Eiroa [19] formulated thin-shell wormholes in the scenario of generalized Chaplygin gas and found more unstable static solutions. Also, Gorini et al. [20, 21] investigated the Tolman-Oppenheimer-Volkoff equations and found the wormhole like solutions with a spacetime singularity for a model filled with the Chaplygin gas and generalized Chaplygin gas (GCG).

It has been established that our universe is dominated by dark energy

which is responsible for the continuous acceleration of the universe. There are many candidates of dark energy such as Chaplygin gas, GCG and modified Chaplygin gas (MCG), etc. In this scenario, Kamenshchik et al. [22] discussed the first ever FRW cosmological model supported by the Chaplygin gas and GCG. The same others [23] explored branes in the background of BTZ and anti de-Sitter Schwarzschild black holes in the context of MCG. The equation of state for the MCG is defined as [24]

$$p = A\sigma - \frac{B}{\sigma^\beta}, \quad (1)$$

where $A > 0$, $B > 0$ and $0 < \beta \leq 1$. A class of Chaplygin gas can be recovered for different choices of parameters A , B and β , such as:

- for $A = 0$, $\beta = 1$, we get usual Chaplygin gas.
- for $A = 0$, it reduces to GCG.
- for $\beta = 1$, it is another form of simple MCG.

In this paper, we construct spherical thin-shell wormholes with MCG as matter located on the shell. The paper is organized as follows. The next section is devoted to provide a general formalism for the construction of spherical thin-shell wormholes. Section 3 deals with the procedure about the stability of static wormhole solutions which is applied to particular examples in section 4. Finally, we conclude the results in the last section.

2 Basic Formalism for Thin-Shell Wormhole

In this section, we develop a general formalism to construct spherical thin-shell wormholes. We take general spherically symmetric spacetime given by

$$ds^2 = -N(r)dt^2 + N^{-1}(r)dr^2 + G(r)(d\theta^2 + \sin^2\theta d\phi^2), \quad (2)$$

where $0 \leq \theta \leq \pi$, $0 \leq \phi < 2\pi$ are the angular coordinates and $N(r)$, $G(r)$ are positive functions of the radial coordinate $r > 0$. The cut and paste technique is an elegant way to construct a thin-shell wormhole solution. For this purpose, we cut the interior region of the manifold (2) with $r < a$, yielding two identical four-dimensional copies \mathcal{V}^\pm with radius $r \geq a$

$$\mathcal{V}^\pm = \{x^\mu = (t, r, \theta, \phi) / r \geq a\}. \quad (3)$$

The assumed radius “ a ” is taken greater than the horizon radius r_h of the manifold (2) to avoid singularities and horizons. We obtain a new manifold by pasting these copies at the timelike hypersurface $\Sigma = \Sigma^\pm = \{r - a = 0\}$, where the boundaries Σ^\pm correspond to \mathcal{V}^\pm . This created manifold $\mathcal{V} = \mathcal{V}^+ \cup \mathcal{V}^-$ is called geodesically complete satisfying the flare-out condition i.e., $G'(a) > 0$, which describes a wormhole having two regions stick with a throat radius a (called minimal surface area). The proper radial distance can be defined on \mathcal{V} as $s = \pm \int_a^r \sqrt{\frac{1}{N(r)}} dr$, which depicts the throat position for $s = 0$, where \pm correspond to \mathcal{V}^\pm .

The intrinsic three-dimensional metric at the throat Σ is given by

$$ds^2 = -d\tau^2 + a^2(\tau)(d\theta^2 + \sin^2\theta d\phi^2), \quad (4)$$

where a is a function of proper time τ . We have applied the Darmois-Israel formalism to the matter at Σ . The extrinsic curvature K_{ij}^\pm associated with the shell is defined as

$$K_{ij}^\pm = -n_\gamma^\pm \left(\frac{\partial^2 x_\pm^\gamma}{\partial \eta^i \partial \eta^j} + \Gamma_{\mu\nu}^\gamma \frac{\partial x_\pm^\mu \partial x_\pm^\nu}{\partial \eta^i \partial \eta^j} \right), \quad (i, j = 0, 2, 3). \quad (5)$$

where 4-vector unit normals n_γ^\pm to \mathcal{V}^\pm are

$$n_\gamma^\pm = \pm \left| g^{\mu\nu} \frac{\partial f}{\partial x^\mu} \frac{\partial f}{\partial x^\nu} \right|^{-\frac{1}{2}} \frac{\partial f}{\partial x^\gamma} = \left(-\dot{a}, \frac{\sqrt{N(r) + \dot{a}^2}}{N(r)}, 0, 0 \right), \quad (6)$$

satisfying the relation $n^\gamma n_\gamma = 1$. Using the orthonormal basis for Eq.(2), $\{e_{\hat{\tau}} = e_\tau, e_{\hat{\theta}} = [G(a)]^{-\frac{1}{2}} e_\theta, e_{\hat{\phi}} = [G(a) \sin^2 \theta]^{-\frac{1}{2}} e_\phi\}$, we obtain the following non-trivial extrinsic curvature components

$$K_{\hat{\tau}\hat{\tau}}^\pm = \mp \frac{N'(a) + 2\ddot{a}}{2\sqrt{N(a) + \dot{a}^2}}, \quad K_{\hat{\theta}\hat{\theta}}^\pm = K_{\hat{\phi}\hat{\phi}}^\pm = \pm \frac{G'(a)}{2G(a)} \sqrt{N(a) + \dot{a}^2}. \quad (7)$$

where dot and prime mean derivatives with respect to τ and r , respectively. The discontinuity in the extrinsic curvatures across a junction surface yields the Lanczos equations on the shell

$$S_{\hat{i}\hat{j}} = \frac{1}{8\pi} \{g_{\hat{i}\hat{j}} K - [K_{\hat{i}\hat{j}}]\}, \quad (8)$$

where $S_{\hat{i}\hat{j}} = \text{diag}(\sigma, p_{\hat{\theta}}, p_{\hat{\phi}})$ is the surface stress-energy tensor which determines the surface stresses of Σ , and $[K_{\hat{i}\hat{j}}] = K_{\hat{i}\hat{j}}^+ - K_{\hat{i}\hat{j}}^-$, $K = \text{tr}[K_{\hat{i}\hat{j}}] = [K_{\hat{i}}^{\hat{i}}]$

provides relations between the extrinsic curvatures. The surface stresses i.e., surface energy density σ and surface pressures $p = p_{\hat{\theta}} = p_{\hat{\phi}}$ to shell with Eqs.(7) and (8) become

$$\sigma = -\frac{G'(a)}{4\pi G(a)}\sqrt{N(a) + \dot{a}^2}, \quad (9)$$

$$p = p_{\hat{\theta}} = p_{\hat{\phi}} = \frac{\sqrt{N(a) + \dot{a}^2}}{8\pi} \left[\frac{2\ddot{a} + N'(a)}{N(a) + \dot{a}^2} + \frac{G'(a)}{G(a)} \right]. \quad (10)$$

Inserting the above equations in Eq.(1), we obtain a second order differential equation describing the evolution of the wormhole throat

$$\begin{aligned} & \{ [2\ddot{a} + N'(a)] G(a) + [(N(a) + \dot{a}^2) (1 + 2A)] G'(a) \} [G'(a)]^\beta \\ & - 2B(4\pi G(a))^{1+\beta} [N(a) + \dot{a}^2]^{\frac{1-\beta}{2}} = 0. \end{aligned} \quad (11)$$

3 Stability Analysis and Linear Perturbations

In this section, we investigate stability of wormhole static solutions through linear perturbations [14]. We consider static configuration ($\dot{a} = \ddot{a} = 0$) of surface stresses (energy density, surface pressure) and dynamical equation of wormhole from Eqs.(9)-(11) as

$$\sigma_0 = -\frac{\sqrt{N(a_0)} G'(a_0)}{4\pi G(a_0)}, \quad p_0 = \frac{\sqrt{N(a_0)}}{8\pi} \left[\frac{N'(a_0)}{N(a_0)} + \frac{G'(a_0)}{G(a_0)} \right], \quad (12)$$

$$\begin{aligned} & \{ G'(a_0)N'(a_0) + G'(a_0)N(a_0) (1 + 2A) \} [G'(a_0)]^\beta \\ & - 2B(4\pi G(a_0))^{1+\beta} [N(a_0)]^{\frac{1-\beta}{2}} = 0. \end{aligned} \quad (13)$$

The conservation equation with Eqs.(9) and (10) can be defined as

$$\frac{d}{d\tau}(\sigma\Delta) + p\frac{d\Delta}{d\tau} = \{ [G'(a)]^2 - 2G(a)G''(a) \} \left\{ \frac{\dot{a}\sqrt{N(a) + \dot{a}^2}}{2G(a)} \right\}, \quad (14)$$

where $\Delta = 4\pi G(a)$ gives the wormhole throat area. The left hand side of the above equation describes the rate of change of throat internal energy and

throat's internal forces work done. Using wormhole throat area definition and Eq.(9), the above equation becomes

$$G(a)\dot{\sigma} + G'(a)\dot{a}(\sigma + p) = - \{[G'(a)]^2 - 2G(a)G''(a)\} \left\{ \frac{\dot{a}\sigma}{2G'(a)} \right\}, \quad (15)$$

which further reduces to

$$G(a)\sigma' + G'(a)(\sigma + p) + \{[G'(a)]^2 - 2G(a)G''(a)\} \left\{ \frac{\sigma}{2G'(a)} \right\} = 0, \quad (16)$$

where we have used $\sigma' = \frac{\dot{\sigma}}{\dot{a}}$. It is noted from Eq.(1) that p is a function of σ . Thus, the above equation is a first order differential equation in $\sigma(a)$ and can be written as $\sigma'(a) = H(a, \sigma(a))$. This equation yields a unique solution for a given initial condition such that H has continuous partial derivative. The integration of Eq.(16) gives $\sigma(a)$, thus the thin-shell equation of motion describing the throat dynamics can be obtained from Eq.(9) as

$$\dot{a}^2 + \Phi(a) = 0. \quad (17)$$

where the potential function $\Phi(a)$ is defined by

$$\Phi(a) = N(a) - 16\pi^2 \left[\frac{G(a)}{G'(a)} \sigma(a) \right]^2. \quad (18)$$

For the stability analysis of static solutions under the radial perturbations, we expand the potential function $\Phi(a)$ by Taylor series expansion around $a = a_0$ upto second order as

$$\Phi(a) = \Phi(a_0) + \Phi'(a_0)(a - a_0) + \frac{1}{2}\Phi''(a_0)(a - a_0)^2 + O[(a - a_0)^3]. \quad (19)$$

The existence and stability of static solution depend upon the inequalities $a_0 > r_h$ and $\Phi''(a_0) \leq 0$, $\Phi(a_0) = 0 = \Phi'(a_0)$, respectively. The solution will be stable or unstable, if $\Phi''(a_0) > 0$ or $\Phi''(a_0) < 0$, respectively. The first derivative of potential function with Eq.(16) becomes

$$\Phi'(a) = N'(a) + 16\pi^2 \sigma(a) \frac{G(a)}{G'(a)} [\sigma(a) + 2p(a)]. \quad (20)$$

Also, from Eq.(1), we have

$$p'(a) = \sigma'(a) \left[(1 + \beta)A - \frac{\beta p(a)}{\sigma(a)} \right], \quad (21)$$

and would be written as

$$\sigma'(a) + 2p'(a) = \sigma'(a) \left[1 + 2\left\{ (1 + \beta)A - \frac{\beta p(a)}{\sigma(a)} \right\} \right]. \quad (22)$$

Using the above equation and Eq.(16), the second derivative of potential function yields

$$\begin{aligned} \Phi''(a) &= N''(a) - 8\pi^2 \left\{ [\sigma(a) + 2p(a)]^2 + 2\sigma(a) \left[\left(\frac{3}{2} - \frac{G(a)G''(a)}{[G'(a)]^2} \right) \sigma(a) \right. \right. \\ &\quad \left. \left. + p(a) \left[1 + 2 \left((1 + \beta)A - \frac{\beta p(a)}{\sigma(a)} \right) \right] \right] \right\}. \end{aligned} \quad (23)$$

Using Eq.(12), it follows that

$$\begin{aligned} \Phi''(a_0) &= N''(a_0) + \frac{(\beta - 1)[N'(a_0)]^2}{2N(a_0)} + N'(a_0) [(1 - \beta + 2A(1 + \beta)) \\ &\quad \times \frac{G'(a_0)}{2G(a_0)} + \beta \frac{G''(a_0)}{G'(a_0)}] + (1 + 2A)(1 + \beta) \left[\frac{G'''(a_0)}{G'(a_0)} \right. \\ &\quad \left. - \left(\frac{G'(a_0)}{G(a_0)} \right)^2 \right] N(a_0). \end{aligned} \quad (24)$$

4 Applications to Particular Examples

In this section, we apply the general formalism developed in the above sections for the construction and stability of spherical thin-shell wormholes to Reissner-Nordström (RN), Schwarzschild de-Sitter and anti de-Sitter geometries.

4.1 Reissner-Nordström Wormholes

Here, we formulate the RN wormholes and investigate their stability. The metric functions for RN have the form

$$N(r) = 1 - \frac{2M}{r} + \frac{Q^2}{r^2}, \quad G(r) = r^2, \quad (25)$$

where M , Q are the mass and charge associated with the RN geometry. The inner $(-)$ and outer $(+)$ horizons for $0 < |Q| < M$ turn out to be

$$r^\pm = M \pm \sqrt{M^2 - Q^2}. \quad (26)$$

The extremal black hole is obtained for $|Q| = M$, while a naked singularity is formed for $|Q| > M$. For the RN wormhole, the condition $a_0 > r_h = r^+$ must be satisfied. The surface energy density and surface pressure for the RN wormhole solution becomes

$$\sigma_0 = -\frac{\sqrt{a_0^2 - 2Ma_0 + Q^2}}{2\pi a_0^2}, \quad p_0 = \frac{a_0 - M}{4\pi a_0 \sqrt{a_0^2 - 2Ma_0 + Q^2}}. \quad (27)$$

The dynamical equation satisfied by the throat radius is obtained by substituting Eq.(25) in (13)

$$a_0^2(1 + 2A) - (1 + 4A)a_0M + 2AQ^2 - 2B(2\pi)^{1+\beta} a_0^{2+2\beta} (a_0^2 - 2Ma_0 + Q^2)^{\frac{1-\beta}{2}} = 0. \quad (28)$$

Also, the potential function with Eqs.(24) and (25) can be written as

$$\begin{aligned} \Phi''(a_0) &= \frac{1}{a_0^4(a_0^2 - 2Ma_0 + Q^2)} \left\{ -2 \left[(1 + \beta) (a_0^4(1 + 2A) + 4AQ^4 \right. \right. \\ &\quad - 10Aa_0^3M - 14a_0AMQ^2 + (3 + 12A)a_0^2M^2 + 6Aa_0^2Q^2) \\ &\quad \left. \left. - a^3M(3 + 4\beta) - a_0MQ^2(1 + 2\beta) + 2\beta a_0^2Q^2 \right] \right\}. \quad (29) \end{aligned}$$

We solve Eq.(28) for a_0 numerically with different values of $0 < \beta \leq 1$. The resulting solution is substituted in Eq.(29) in order to check whether the solution is stable or unstable depending upon $\Phi''(a_0) > 0$ or $\Phi''(a_0) < 0$, respectively. The stable and unstable static solutions are represented by the black and dotted curves, respectively. We can summarize the results in Figures **1-3** for RN wormholes as follows:

- In Figure **1** when $\beta = 0.2$, there exists one unstable static solution corresponding to $\frac{|Q|}{M} = 0, 0.7$ and two unstable and one stable solution for $\frac{|Q|}{M} = 0.999$. The throat radius in each case decreases for large value of $BM^{\beta+1}$ which touches the horizon radius of the given manifold. Also, the horizon radius decreases and eventually disappears for large values of charge. For $\frac{|Q|}{M} = 1.1$, there are three solutions two of them are unstable and one is stable.
- When $\beta = 0.6$ (Figure **2**), there exists one unstable static solution corresponding to $\frac{|Q|}{M} = 0, 0.7, 1.1$, while two unstable and one stable solution for $\frac{|Q|}{M} = 0.999$. The throat radius has similar behavior as in the above case.

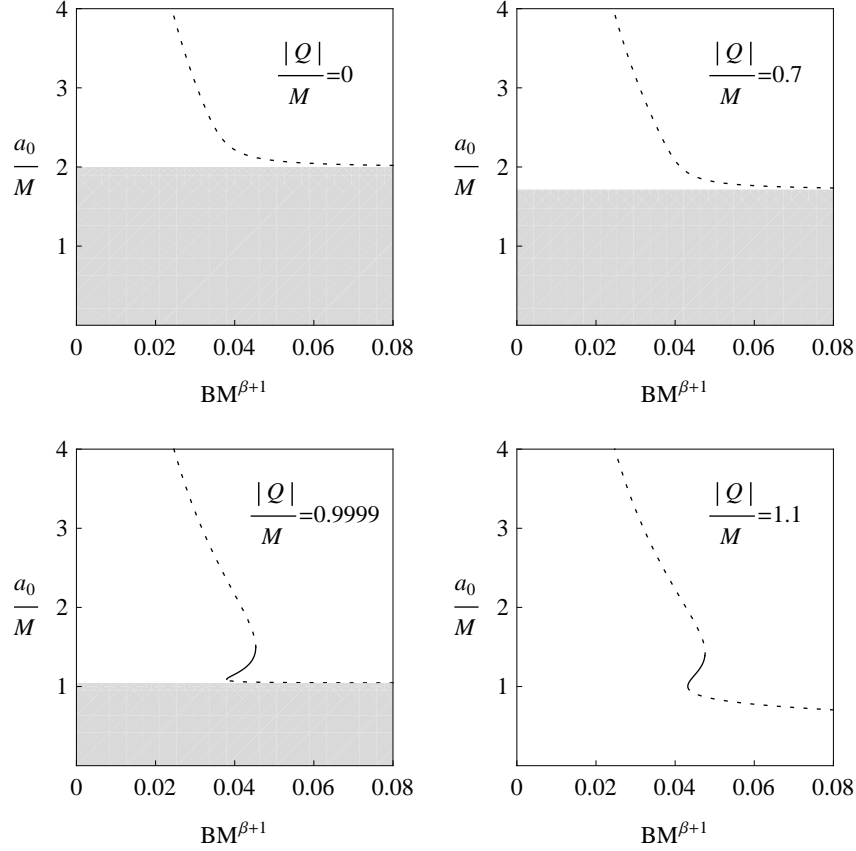


Figure 1: RN thin-shell wormholes under radial perturbations with $\beta = 0.2$, $A = 1$ and different values of $\frac{|Q|}{M}$. The solid and dotted curves represent stable and unstable solutions respectively, and the grey zones correspond to the non-physical regions, where $a_0 \leq r_h$.

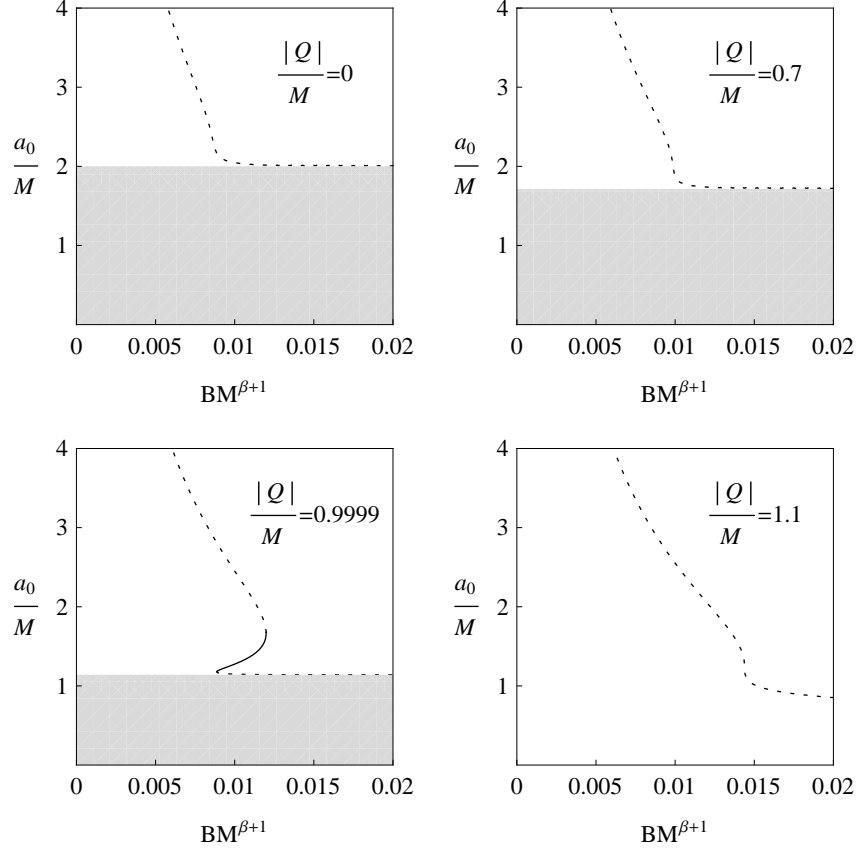


Figure 2: RN thin-shell wormholes for $\beta = 0.6$, $A = 1$ with different values of $\frac{|Q|}{M}$.

- When $\beta = 1$ (Figure 3), there exist both stable and unstable static solutions for $0 < \frac{|Q|}{M} < 1$, while only unstable solution for $\frac{|Q|}{M} > 1$.

We would like to mention here that our results for $\beta = 0.2$ are similar to that reported in [19] for $\frac{|Q|}{M} = 0, 0.7, 0.999$, whereas for $\frac{|Q|}{M} = 1.1$, we have one extra unstable solution. When $\beta = 0.6$, we have only one unstable solution for $\frac{|Q|}{M} = 1.1$. Similarly, for $\beta = 1$, we have one more stable solution for $\frac{|Q|}{M} = 0, 0.7$ and only unstable for $\frac{|Q|}{M} = 1.1$.

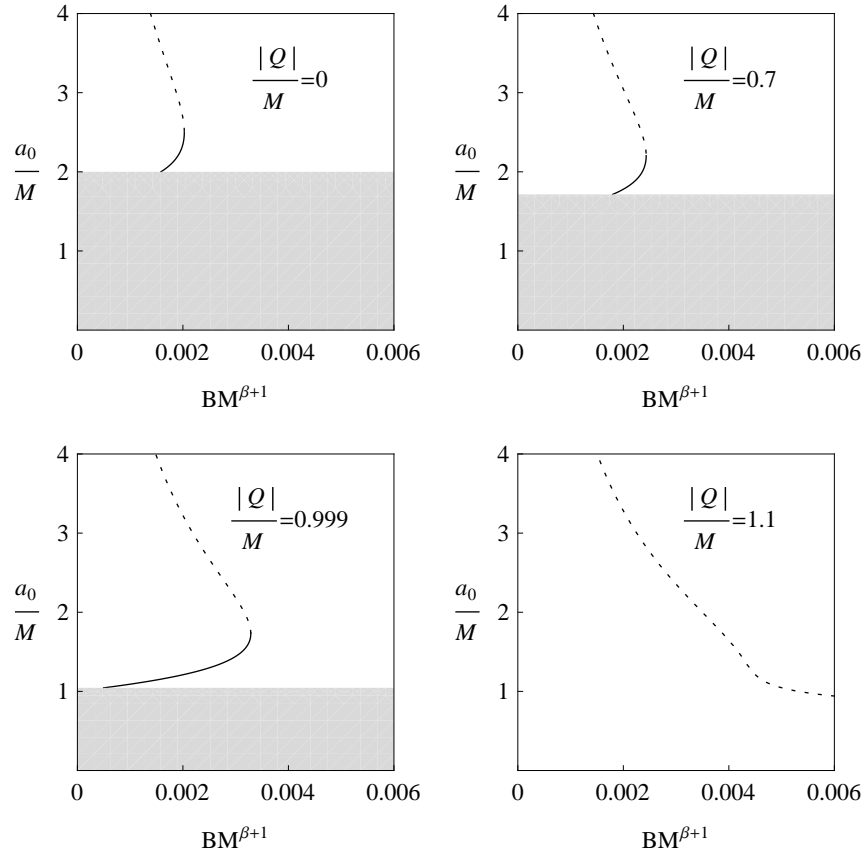


Figure 3: RN thin-shell wormholes for $\beta = 1$, $A = 1$ with different values of $\frac{|Q|}{M}$.

4.2 Schwarzschild de-Sitter and anti de-Sitter Wormholes

For the Schwarzschild de-Sitter and anti de-Sitter thin-shell wormholes, the metric functions have the following form

$$N(r) = 1 - \frac{2M}{r} - \frac{\Lambda r^2}{3}, \quad G(r) = r^2, \quad (30)$$

where $\Lambda > 0$ is the cosmological constant. The function $N(r)$ remains negative for $\Lambda M^2 > \frac{1}{9}$, while for $0 < \Lambda M^2 \leq \frac{1}{9}$, the Schwarzschild de-Sitter geometry has two horizons event r_h and cosmological r_c as follows

$$r_h = \frac{-1 + i\sqrt{3} - (1 + i\sqrt{3})(-3\sqrt{\Lambda}M + i\sqrt{1 - 9\Lambda M^2})^{\frac{2}{3}}}{2\sqrt{\Lambda}(-3\sqrt{\Lambda}M + i\sqrt{1 - 9\Lambda M^2})^{\frac{1}{3}}}, \quad (31)$$

$$r_c = \frac{1 + (-3\sqrt{\Lambda}M + i\sqrt{1 - 9\Lambda M^2})^{\frac{2}{3}}}{\sqrt{\Lambda}(-3\sqrt{\Lambda}M + i\sqrt{1 - 9\Lambda M^2})^{\frac{1}{3}}}. \quad (32)$$

The horizons r_h and r_c are increasing and decreasing function of Λ , since $\lim_{\Lambda \rightarrow 0^+} r_h = 2M$. Moreover, $\lim_{\Lambda \rightarrow 0^+} r_c = +\infty$ and $r_h = r_c = 3M$ for $\Lambda M^2 = \frac{1}{9}$, which is not possible in wormhole configuration. Thus the static solution will exist if $0 < \Lambda M^2 < \frac{1}{9}$ and $r_h < a_0 < r_c$. The event horizon r'_h for the Schwarzschild anti de-Sitter geometry is given by

$$r'_h = \frac{1 - (-3\sqrt{|\Lambda|}M + \sqrt{1 + 9|\Lambda|M^2})^{\frac{2}{3}}}{\sqrt{|\Lambda|}(-3\sqrt{|\Lambda|}M + \sqrt{1 + 9|\Lambda|M^2})^{\frac{1}{3}}}, \quad (33)$$

which is continuous and increasing function of Λ , as $\lim_{\Lambda \rightarrow 0^-} r'_h = 2M$ and $\lim_{\Lambda \rightarrow -\infty} r'_h = 0$. This shows that r'_h has values in the range $0 < r'_h < 2M$ and the static solution will exist whenever $a_0 > r'_h$. The corresponding surface energy density and pressure at the throat become

$$\sigma_0 = -\frac{\sqrt{3a_0 - 6M - \Lambda a_0^3}}{2\pi a_0 \sqrt{3a_0}}, \quad p_0 = \frac{3a_0 - 3M - 2\Lambda a_0^3}{4\pi a_0 \sqrt{3a_0(3a_0 - 6M - \Lambda a_0^3)}}. \quad (34)$$

The dynamical equation and potential function from Eqs.(13) and (24) with (30) yield

$$\begin{aligned} & a_0(1 + 2A) - (1 + 4A)M - \frac{2}{3}\Lambda a_0^3(1 + A) - 2B(2\pi)^{1+\beta} a_0^{\frac{3(1+\beta)}{2}} \\ & \times \left(a_0 - 2M - \frac{\Lambda}{3}a_0^3\right)^{\frac{1-\beta}{2}} = 0. \end{aligned} \quad (35)$$

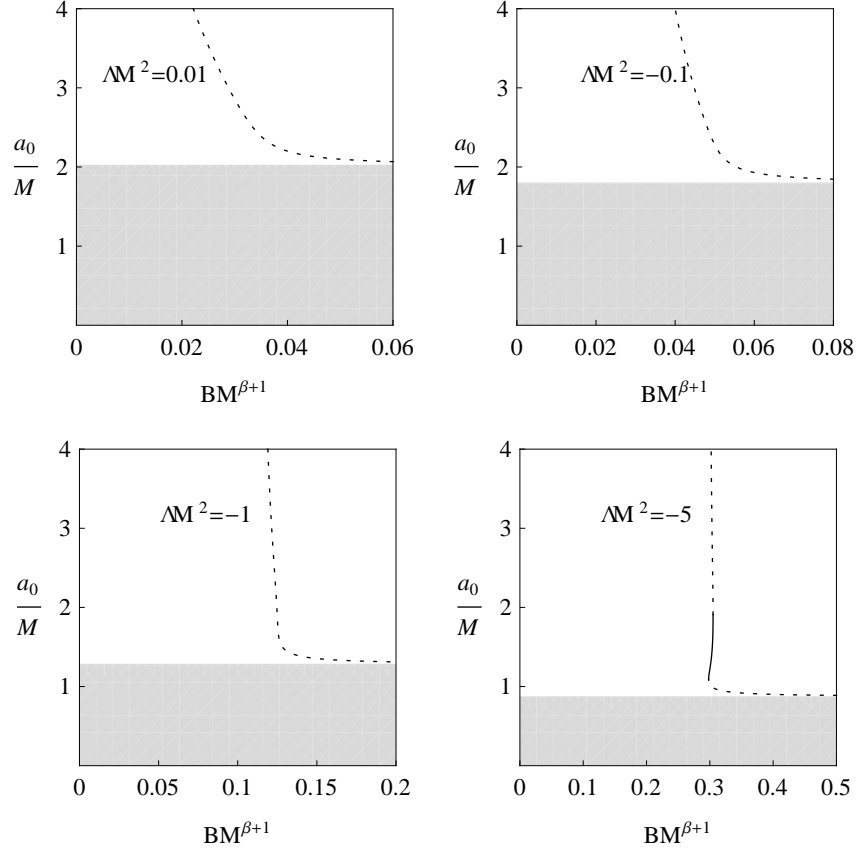


Figure 4: Schwarzschild de-Sitter and anti de-Sitter thin-shell wormholes under radial perturbations with parameters $\beta = 0.2$, $A = 1$, ΛM^2 . The solid and dotted curves indicate the stable and unstable solutions respectively, and the grey zones correspond to the non-physical regions, where $a_0 \leq r_h$.

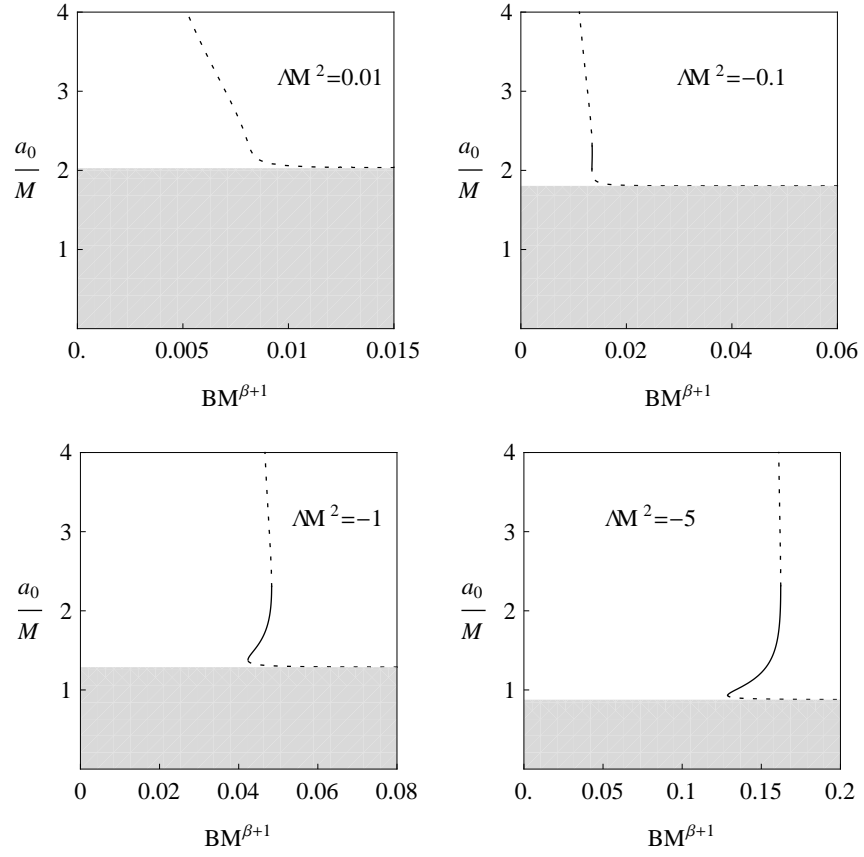


Figure 5: Schwarzschild de-Sitter and anti de-Sitter thin-shell wormholes with $\beta = 0.6$, $A = 1$, ΛM^2 .

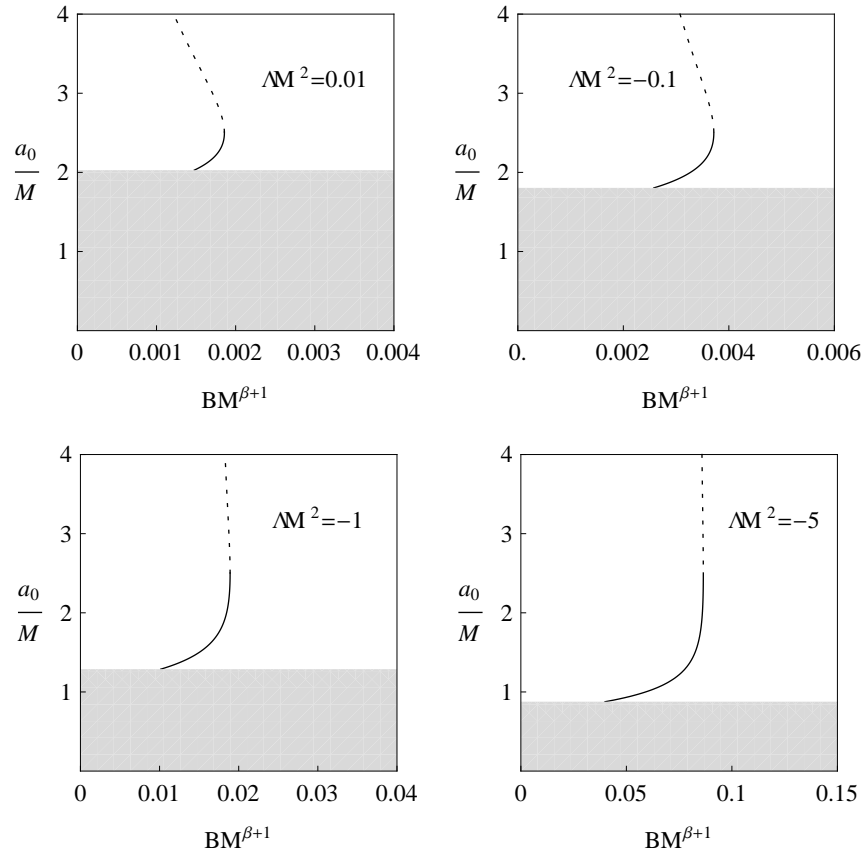


Figure 6: Schwarzschild de-Sitter and anti de-Sitter thin-shell wormholes with $\beta = 1$, $A = 1$, ΛM^2 .

$$\begin{aligned}
\Phi''(a_0) &= \frac{2}{a_0^3(\Lambda a_0^3 - 3a_0 + 6M)} \left\{ (1 + \beta) [3a_0^2(1 + 2A) + 9M^2(1 + 4A)] \right. \\
&\quad - 30a_0AM + 6a_0^3\Lambda AM - 2A\Lambda a_0^4 - 3a_0M(3 + 4\beta) \\
&\quad \left. - 2a_0^4\beta\Lambda + 3a_0^3\Lambda M(2\beta - 1) \right\}. \tag{36}
\end{aligned}$$

Similar to the RN case, we solve Eq.(35) numerically for a_0 and explore its stability. The results are shown in Figures 4-6 for $0 < \beta \leq 1$ with different values of parameters.

- In Figure 4 when $\beta = 0.2$, there exists one unstable static solution corresponding to $\Lambda M^2 = 0.01, -0.1, -1$, while two unstable and one stable solution for $\Lambda M^2 = -5$. Also, the throat radius decreases and touches the horizon radius for large value of $BM^{\beta+1}$.
- When $\beta = 0.6$ (Figure 5), one unstable static solution corresponds to $\Lambda M^2 = 0.01$, one stable and two unstable for $\Lambda M^2 = -0.1, -1, -5$.
- In Figure 6 ($\beta = 1$), there exist both stable and unstable solutions for each case corresponding to $\Lambda M^2 = 0.01, -0.1, -1, -5$.

In this case, we have also found some extra solutions for the MCG. Notice that all the solutions are of unstable type for $\beta = 0.2$ with different values of ΛM^2 [19]. On the other hand, we have found two extra stable static solutions for $\Lambda M^2 = -5$. Similarly, for $\beta = 0.6$, there exist two extra stable and unstable solutions for $\Lambda M^2 = -0.1, -1$. For $\beta = 1$, we have two extra stable solutions for $\Lambda M^2 = 0.01, -0.1$, whereas for $\Lambda M^2 = -1, -5$, we have similar solutions to [19].

5 Conclusions

In this paper, we have found a class of spherical thin-shell wormholes with cut and paste technique. We have assumed MCG to deal with the exotic matter located in the wormhole throat Σ . The Darmois-Israel formalism has been used to find the surface energy density and pressure. We have manipulated the results numerically and adopted the standard potential approach to investigate stability of the static wormhole solutions. The results representing the stable and unstable solutions with solid and dotted curves, respectively are shown in Figures 1-6. In particular, we have explored stability of RN as well as Schwarzschild de-Sitter and anti-de-Sitter thin-shell wormholes for

different values of the gas exponent β and compared our results with those already found in [19] for the generalized Chaplygin gas. It is concluded that some extra stable as well as unstable static solutions exist depending upon the parameters A , B , β , $\frac{|Q|}{M}$, ΛM^2 involving in the model. This shows that the choice of equation of state plays a vital role in the existence of wormhole solutions. We would like to mention here that all our results reduce to that of [19] when we take $A = 0$.

Acknowledgments

We would like to thank the Higher Education Commission, Islamabad, Pakistan, for its financial support through the *Indigenous Ph.D. 5000 Fellowship Program Batch-VII*. One of us (MA) would like to thank University of Education, Lahore for the study leave.

References

- [1] Morris, M. and Thorne, K.: Am. J. Phys. **56**(1988)395.
- [2] Visser, M.: *Lorentzian Wormholes* (AIP Press, New York, 1996).
- [3] Visser, M., Kar, S. and Dadhich, N.: Phys. Rev. Lett. **90**(2003)201102.
- [4] Visser, M.: Phys. Rev. D **39**(1989)3182; Nucl. Phys. B **328**(1989)203.
- [5] Darmois, G.: Memorial des Sciences Mathematiques (Gauthier-Villars, 1927) Fasc. 25; Israel, W.: Nuovo Cimento B **44S10**(1966)1; ibid Erratum **B48**(1967)463.
- [6] Musgrave, P. and Lake, K.: Class. Quantum Grav. **13**(1996)1885.
- [7] Rahaman, F., Kalam, M., Rahman, K.A. and Chakraborti, S.: Gen. Relativ. Gravit. **39**(2007)945.
- [8] Lemos, J.P.S. and Lobo, F.S.N.: Phys. Rev. D **78**(2008)044030.
- [9] Dias, G.A.S. and Lemos, J.P.S.: Phys. Rev. D **82**(2010)084023.
- [10] Rahaman, F., Kuhfittig, P.K.F., Kalam, M., Usmani, A.A. and Ray, S.: Class. Quantum Grav. **28**(2011)155021.

- [11] Poisson, E and Visser, M.: Phys. Rev. D **52**(1995)7318.
- [12] Eiroa, E.F. and Romero, G.E.: Gen. Relativ. Gravit. **36**(2004)651.
- [13] Lobo, F.S.N. and Crawford, P.: Class. Quantum Grav. **21**(2004)391.
- [14] Eiroa, E.F. and Simeone, C.: Phys. Rev. D **71**(2005)127501; Eiroa, E.F.: Phys. Rev. D **78**(2008)024018; Rahaman, F., Rahman, Sk.A., Rakib, A. and Kuhfitting, Peter K.F.: Int. J. Theor. Phys. **49**(2010)2364; Bejarano, C. and Eiroa, E.F.: Phys. Rev. D **84**(2011)064043.
- [15] Eiroa, E.F. and Simeone, C.: Phys. Rev. D **70**(2004)044008; *ibid* **81**(2010)084022; Bejarano, C., Eiroa, E.F. and Simeone, C.: Phys. Rev. D **75**(2007)027501.
- [16] Sharif, M. and Azam, M.: J. Phys. Soc. Jpn. **81**(2012)124006; JCAP **04**(2013)023; Eur. Phys. J. C **73**(2013)2407.
- [17] Eiroa, E.F. and Simeone, C.: Phys. Rev. D **76**(2007)024021.
- [18] Bandyopadhyay, T., Baveja, A. and Chakraborty, S.: Int. J. Mod. Phys. D **13**(2009)1977.
- [19] Eiroa, E.F.: Phys. Rev. D **80**(2009)044033.
- [20] Gorini, V., Moschella, U., Kamenshchik, A.Yu., Pasquier, V. and Starobinsky, A.A.: Phys. Rev. D **78**(2008)064064.
- [21] Gorini, V., Kamenshchik, A.Yu., Moschella, U., Piattella, O.F. and Starobinsky, A.A.: Phys. Rev. D **80**(2009)104038.
- [22] Kamenshchik, A.Yu., Moschella, U. and Pasquier, V.: Phys. Lett. B **511**(2001)265.
- [23] Kamenshchik, A.Yu., Moschella, U. and Pasquier, V.: Phys. Lett. B **487**(2000)7.
- [24] Chimento, L.P.: Phys. Rev. D **69**(2004)123517.